Trapping and Manipulation of Isolated Atoms Using Nanoscale Plasmonic Structures

Trapping and Manipulation of Isolated Atoms Using Nanoscale Plasmonic Structures

D. E. Chang,[1] J. D. Thompson,[2] H. Park,[2,3] V. Vuletić,[4] A. S. Zibrov,[2] P. Zoller,[5] and M. D. Lukin[2]

[1]*Center for the Physics of Information and Institute for Quantum Information, California Institute of Technology, Pasadena, California 91125, USA*

[2]*Department of Physics, Harvard University, Cambridge, Massachusetts 02138, USA*

[3]*Department of Chemistry and Chemical Biology, Harvard University, Cambridge, Massachusetts 02138, USA*

[4]*Department of Physics, MIT-Harvard Center for Ultracold Atoms, and Research Laboratory of Electronics, Massachusetts Institute of Technology, Cambridge, Massachusetts 02139, USA*

[5]*Institute for Quantum Optics and Quantum Information of the Austrian Academy of Sciences, A-6020 Innsbruck, Austria*

(Received 26 May 2009; published 17 September 2009)

We propose and analyze a scheme to interface individual neutral atoms with nanoscale solid-state systems. The interface is enabled by optically trapping the atom via the strong near-field generated by a sharp metallic nanotip. We show that under realistic conditions, a neutral atom can be trapped with position uncertainties of just a few nanometers, and within tens of nanometers of other surfaces. Simultaneously, the guided surface plasmon modes of the nanotip allow the atom to be optically manipulated, or for fluorescence photons to be collected, with very high efficiency. Finally, we analyze the surface forces, heating and decoherence rates acting on the trapped atom.

DOI: 10.1103/PhysRevLett.103.123004 PACS numbers: 37.10.Gh, 42.50.−p, 73.20.Mf, 78.67.Bf

Much interest has recently been directed towards hybrid systems that integrate isolated atomic systems with solid-state devices [1–4]. These efforts are aimed at combining the excellent coherence and control possible with isolated atoms, ions and molecules, with the miniaturization and integrability of solid-state devices. A key ingredient is the ability to trap, coherently manipulate, and measure individual cold atoms within ~100 nm of a surface.

Here, we describe a technique that allows a single atom to be optically trapped within a nanoscale region above the surface of a sharp, conducting nanotip. Under illumination with a single blue-detuned laser beam, the nanotip behaves as a ''lightning rod'' that generates very large field gradients and creates an intensity minimum that can be used to tightly trap an atom. Simultaneously, the trapped atom can efficiently couple to guided surface plasmon modes of the tip, which enables efficient fluorescence collection, optical manipulation and strong coupling at the single-photon level [5–7].

The trapping technique described here might enable several unique applications. For example, single atoms could be deterministically positioned near micro- and nanophotonic structures [8–10] [see Fig. 1(a)]. Alternatively, hybrid quantum systems consisting of single atoms or molecules near charged or magnetized solid-state quantum systems could be realized, enabling direct strong electrical or magnetic coupling [11]. Finally, a trapped atom might be used as a novel scanning probe for sensing magnetic or electric fields with nanoscale resolution. We note that forces associated with metallic systems are being actively explored, in the context of optical tweezers for dielectric objects on surfaces [12] and electro-optical atomic trapping using nanotubes [13]. In contrast to the latter work, our scheme offers an all-optical trapping method, an open geometry [14], and an efficient mechanism for optical readout and manipulation.

We first derive the optical trapping potential for an atom near a nanotip, whose surface is parameterized by a paraboloid of revolution with rotational axis along z, $z(\rho) = -z_0 + \rho^2/4z_0$ (the offset $-z_0$ is conventional in a paraboloidal coordinate transformation). Here z_0 characterizes the curvature of the tip and $\rho = \sqrt{x^2 + y^2}$ is the radial coordinate [see Fig. 1(b) for an illustration of a tip with $z_0 = 2$ nm). We consider the total field produced by a plane wave incident from the far field, $\mathbf{E}_{\text{inc}}(\mathbf{r}) = E_0 e^{ik_L x - i\omega_L t}\hat{z}$, which is polarized along the nanotip axis. While an exact analytical solution cannot be obtained, the near field around a subwavelength nanotip can be approximated using electrostatic equations that do admit analytical solutions [5]. Within this approximation, the total field outside the nanotip is

$$\mathbf{E}_{\text{total}} = E_0\left(1 + \frac{z_0}{r}(\epsilon_L - 1)\right)\hat{z} + \frac{E_0 z_0}{r(r-z)}(1 - \epsilon_L)\boldsymbol{\rho}, \quad (1)$$

while the field inside the nanotip is uniformly $\mathbf{E}_{\text{total}} = E_0\hat{z}$. Here, $\epsilon_L \equiv \epsilon(\omega_L)$ is the dimensionless electric permittivity of the nanotip at the laser frequency (we assume that the surrounding material is vacuum, $\epsilon = 1$) and $r = \sqrt{\rho^2 + z^2}$. When the nanotip is conducting and far below its plasma resonance, such that $\epsilon_L \ll -1$, the field $\mathbf{E}_{\text{total}} = \epsilon_L E_0\hat{z}$ at the tip end is greatly enhanced and out of phase relative to the incident field. This is essentially the ''lightning rod'' effect of a good conductor [15]. The total field is zero on-axis at $z_{\text{trap}} = z_0(\epsilon_L - 1)$, and relaxes to E_0 far from the tip. A small residual field remains if ϵ_L has a small imaginary component ($\epsilon_L \approx -30 + 0.4i$ in silver at wavelength $\lambda_L = 780$ nm [16]).

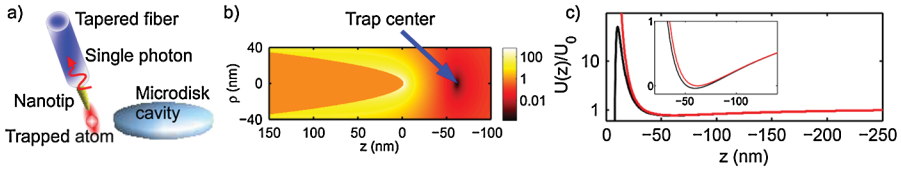

FIG. 1 (color). (a) Schematic of a single atom tightly trapped near a conducting nanotip. The atom is strongly coupled to single surface plasmons guided by the nanotip, which can be efficiently converted to a single photon in a coupled optical fiber, allowing for efficient manipulation and readout. The atom can be brought within tens of nanometers of other surfaces, which allows it to be interfaced, e.g., with an optical microdisk cavity as shown here. (b) Illustration of a nanotip with $z_0 = 2$ nm and normalized total field intensity $|E_{\text{total}}/E_0|^2$. (c) Typical optical potential (red) and total potential (including van der Waals potential, black) for a Rb atom trapped near a $z_0 = 2$ nm nanotip. The potentials are normalized by $U_0 = \hbar\Omega_0^2/\delta$, the optical potential at infinity. The inset shows the potentials around the trap center in greater detail.

For a simple two-level atom, the field minimum provides a trapping potential when the laser is blue-detuned from the transition frequency ω_a ($\delta \equiv \omega_L - \omega_a > 0$), such that the atomic polarizability is negative. Expanding the fields linearly around the trap center, the potential corresponds to that of a harmonic oscillator, whose trapping frequency $\omega_{T,z}$ along z is given by

$$\hbar\,\omega_{T,z} = 2\sqrt{\frac{\hbar\Omega_0^2}{\delta}E_R'}, \tag{2}$$

where $E_R' = E_R(k_a z_{\text{trap}})^{-2}$ is an effective "enhanced" recoil energy relative to the recoil energy $E_R = \hbar^2 k_a^2/2m$ in free space, m is the mass of the atom, $k_a = \omega_a/c$, and Ω_0 is the Rabi frequency associated with the incident field amplitude. The ground-state uncertainty of the trap along z is $a_z = \sqrt{\hbar/2m\omega_{T,z}}$, while the trap frequency in the radial directions is $\omega_{T,\rho} = \omega_{T,z}/2$. Note that the field gradients created by the nanotip strongly enhance E_R', such that larger trap frequencies $\omega_{T,z} \propto 1/|z_{\text{trap}}|$ can be obtained for a given input intensity.

A trapped atom can be optically manipulated and read out via efficient coupling to guided surface plasmons (SPs) that propagate along the nanotip surface. Following the ideas of Ref. [17], a large coupling strength between a single SP (i.e., a single photon) and single atom results when the atom is placed within the SP evanescent field, due to the subdiffraction limit confinement of the SPs. This yields an enhanced spontaneous emission rate Γ_{pl} into the SPs over the rate Γ' into all other channels, which can be characterized by an "effective Purcell factor" $P = \Gamma_{\text{pl}}/\Gamma'$. The Purcell factor for an atom (emission wavelength $\lambda_a = 780$ nm) at position $z = z_{\text{trap}}$ near a silver nanotip is plotted in Fig. 2(a) as a function of z_0. The strong coupling regime $P > 1$ can be achieved over a realistic range of z_0. Furthermore, the coupling is broadband and due only to the small tip size, and thus no tuning of the nanotip is required for different atomic species.

Surface effects can play an important role in the trap characteristics, since for realistic parameters, the distance $d = |\epsilon_L| z_0$ between the trap center and tip surface is on the order of tens of nanometers [see Fig. 2(a)]. Here we analyze several common effects: an attractive van der Waals force from the nanotip, "patch potentials" caused by adatoms that modify the total potential experienced by the atom, and "polarization noise" in the nanotip that induces both motional heating and hyperfine state flips in a multilevel atom. The van der Waals force can be calculated classically based on the interaction between an oscillating dipole and its own reflected field [18]. Taking the known result for the field reflected from a nanotip [5], the van der Waals potential as $z \to -z_0$ is given for a two-level atom by $U_{\text{vdW}}(z) \approx -\frac{3\hbar\Gamma_0}{32k_a^3 d^3}$, where Γ_0 is the free-space spontaneous emission rate. For sufficiently weak optical potentials, the total potential $U_{\text{opt}} + U_{\text{vdW}}$ may cease to support a trapping minimum. The condition for a trap to exist is approximately

$$\frac{\Omega_0^2}{\delta} \gtrsim \frac{9\Gamma_0}{32(k_a|z_{\text{trap}}|)^3}; \tag{3}$$

i.e., the strength of the laser potential should roughly exceed that of the van der Waals force at the trap position. Even if the condition above is satisfied, some probability remains for the atom to tunnel from the local trapping minimum to the surface. However, the tunneling rate is

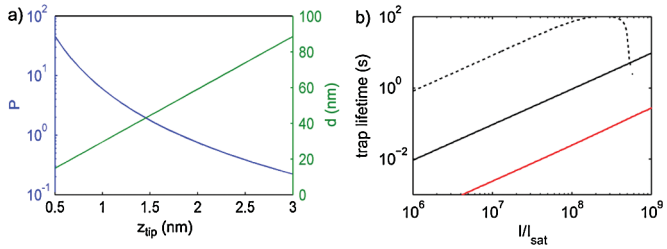

FIG. 2 (color). (a) Purcell factor P (averaged over dipole orientations, blue curve) and trap distance to surface d (green curve) for a ^{87}Rb atom trapped near a silver nanotip, as a function of z_0, in absence of van der Waals forces. (b) Trap lifetime for various values of trapping frequency $\omega_{T,z}$ and tip curvature z_0. The incident trap laser intensity is plotted along the horizontal axis, while the detuning is varied to maintain a given value of $\omega_{T,z}$. The black dashed (solid) curve corresponds to $z_0 = 3$ nm and trap frequency of $\omega_{T,z} = 10(100)$ MHz, while the red curve corresponds to $z_0 = 1$ nm and $\omega_{T,z} = 100$ MHz.

exponentially suppressed with barrier height and can be ignored once Eq. (3) is even moderately satisfied.

A second correction to the potential arises from extra atoms adsorbed on the nanotip surface [19]. Each adatom obtains a static electric dipole moment p_0 due to its electronic wave function being pulled into or away from the surface, thus producing a small static electric field. Their combined static field E_p creates an additional ''patch'' potential for the trapped atom, $U_p = -(1/2)\alpha_s E_p^2$, where α_s is the atomic static polarizability. Assuming that a uniform monolayer of adatoms substitute themselves over some portion of the nanotip surface, we find that the maximum force (i.e., in a worst-case scenario) at a distance d away from the nanotip is given by $F_p(d) \lesssim 0.1 \frac{p_0^2 z_0^2 \alpha}{\epsilon_0^2 d^5 a^4}$, where a is the lattice spacing of the nanotip material. For typical dipole moments of $p_0 \sim 1$ Debye, this force introduces negligible shifts of the trap center and thus will be ignored in our calculations.

Equation (3) predicts that the minimum incident intensity needed to support a trap rises rapidly with decreasing nanotip size. However, for sufficiently large intensities the laser power absorbed by the nanotip, as determined by the imaginary part of ϵ_L, will cause it to melt. Assuming that the nanotip has a good thermal contact conductance (e.g., comparable to achievable values for wires in atom chips [20]) with some substrate, we estimate that incident laser intensities exceeding 10 mW/μm^2 can be used for silver nanotips at $\lambda_L = 780$ nm [21]. This sets a lower bound for z_0 of several hundred picometers. An upper bound is set by the validity of our electrostatic calculations. Specifically, in a subwavelength region around the end of the tip, the tip profile must appear ''sharp'' (as defined by having a large aspect ratio $z/2\rho$), and the trap distance should satisfy $k_a d \lesssim 1$. This places an upper limit to z_0 of several nanometers before higher order electrodynamic terms must be included in the electric field calculation.

We now discuss limitations on atomic coherence times and trap lifetimes. First, the proximity to the surface makes the atom susceptible to magnetic field noise $\mathbf{B}_N$ induced by material losses in the nanotip. This field noise couples to the electron spin via the Hamiltonian $V = -\mu_B g_S \mathbf{S} \cdot \mathbf{B}_N(\mathbf{r}, t)$, resulting in incoherent transitions between ground-state hyperfine levels and jumps between trap motional states. Here μ_B is the Bohr magneton and g_S is the electron spin g factor. An analytical solution for $\mathbf{B}_N$ cannot be found for the nanotip. However, to estimate its effect, we can consider an atom sitting a distance d above a semi-infinite substrate of the same permittivity as the nanotip. The hyperfine transition rate $\Gamma_{\Delta F,\mathrm{mag}}$ and motional jump rate $\Gamma_{\mathrm{jump,mag}}$ due to magnetic noise in this case are $\Gamma_{\Delta F,\mathrm{mag}} \propto \frac{(\mu_0 \mu_B g_S)^2}{\hbar^2 \rho d} k_B T$, $\Gamma_{\mathrm{jump,mag}} \propto \Gamma_{\Delta F,m}(a_z/d)^2$ [22] where ρ is the resistivity of the nanotip. We note that the semi-infinite substrate over estimates the amount of polarizable material and that for realistic tips the noise should be reduced by a factor of order $\sim(z_0/z_{\mathrm{trap}})^2$. The hyperfine transitions result only in a loss of internal atomic coherence, since all hyperfine states can be trapped in the optical fields. In the following we assume that the nanotip roughly sits at room temperature, $T \sim 300$ K.

Analogous processes occur due to inelastic scattering of photons from the trapping field. Because of the tight trap confinement, the change in motional state primarily consists of events where a single phonon is added or subtracted, in analogy with heating of ions in the Lamb-Dicke limit [23]. For a two-level system, we find from second-order perturbation theory [24,25] a jump rate

$$\Gamma_{\mathrm{jump,opt}} \approx \Gamma^{(z)}_{\mathrm{total}} \frac{E'_R}{\hbar \omega_{T,z}} \frac{\Omega_0^2}{\delta^2}, \tag{4}$$

where $\Gamma^{(z)}_{\mathrm{total}}$ denotes the total spontaneous emission rate for a dipole oriented along the nanotip axis. Note that the enhanced recoil energy E'_R yields a larger heating rate as compared to free space. Photon scattering also results in hyperfine transitions, which we calculate using analogous techniques [25]. An additional source of heating is laser shot noise, which causes fluctuations in the trap frequency ω_T. For a laser beam focused to $\sim\lambda^2$, however, this heating is smaller than $\Gamma_{\mathrm{jump,opt}}$ by a factor $\sim(a_z/d)^2$.

As a numerical example, we now consider the trapping of individual ^{87}Rb atoms ($\lambda_a \sim 780$ nm for the $D2$ line, $\Gamma_0 \sim 38$ MHz, saturation intensity $I_{\mathrm{sat}} \sim 1.7$ mW/cm^2) near a silver nanotip. For the nanotip heating rates calculated previously, laser intensities of up to $I \sim 10^9 I_{\mathrm{sat}}$ can be realized. In these examples, both the complex value of ϵ_L and the multilevel atomic structure of Rb have been fully accounted for (i.e., the optical interactions include the atomic fine structure, and are averaged over all magnetic states m_F). In Fig. 2(b) we plot the trap lifetime for various values of $\omega_{T,z}$ and z_0. The incident field intensity is shown along the horizontal axis, while the detunings are varied to keep $\omega_{T,z}$ fixed. The black dashed (solid) curve corresponds to a nanotip of $z_0 = 3$ nm and trap frequency of $\omega_{T,z} = 10(100)$ MHz, while the red curve corresponds to $z_0 = 1$ nm and $\omega_{T,z} = 100$ MHz. Note that $\omega_{T,z} = 100$ MHz yields a ground-state localization of $a_z \sim 2$ nm. The van der Waals force is included in the total potential, and the trap lifetime is the time it takes for the atomic energy to exceed the depth of the total potential, using the jump rates calculated previously and assuming a fully harmonic potential. This estimate should remain qualitatively correct for real potentials which are anharmonic far from the center, since the predicted heating rates $dE/dt \sim \hbar \omega_{T,z} \Gamma_{\mathrm{jump}}$ are independent of trap frequencies. In Fig. 2(b), the regime of linear scaling of the lifetime with intensity (keeping $\omega_{T,z}$ fixed) indicates that the heating is dominated by optical scattering as in a conventional optical dipole trap. For the $\omega_{T,z} = 10$ MHz curve, trap lifetimes exceeding $\sim$1 s can be readily achieved, with saturation in the lifetime occurring as heating via magnetic field noise becomes comparable. The decrease in lifetime at larger intensities (and detunings) is due to the frequency depen-

dence of the permittivity ϵ_L and the trap center being pulled closer to the surface. Spin flip times (dominated by magnetic field noise at large detunings $\delta \sim 10^6\Gamma_0$) are conservatively calculated to be around 10 ms using the results obtained for a semi-infinite substrate; however, based on the small solid angle actually spanned by the nanotip, we estimate that times on the order of a second are possible. When the van der Waals potential does not perturb the trap significantly, the trapped atom sits 90 (30) nm from the tip surface for a tip curvature of $z_0 = 3(1)$ nm, with a Purcell factor of $P \sim 0.2(6)$ when averaged over dipole orientations.

Trap loading can be accomplished by starting with an atom in a separate, far-field, red-detuned optical dipole trap a few microns from the nanotip, and transferring it adiabatically to the blue-detuned nanotip trap. If the far-field beam is polarized perpendicular to the nanotip axis (say along $\hat{x}$), a similar analysis as above shows that the total field along the nanotip axis is given by $\mathbf{E}_{\text{total}} = E_0(1 + \frac{1-\epsilon_L}{1+\epsilon_L}\frac{z_0}{|z|})\hat{x}$. Thus, for this polarization, the incident field is only modified at very close distances to the tip of order $z_\perp \sim z_0(\epsilon_L - 1)/(\epsilon_L + 1) \ll |z_{\text{trap}}|$; i.e., the nanotip has a minimal effect on the far-field trap, allowing it to overlap with the intensity minimum of the nanotip trap.

In summary, we have described a technique that allows for nanoscale trapping and efficient optical manipulation of single atoms on a chip. Such a trap should display long trap lifetimes and atomic coherence times, and its open geometry and large depth allow the atom to be brought into close proximity (~50 nm) of other surfaces. This combination of features creates many exciting opportunities. For example, the nanotip could be used to trap atoms within the evanescent fields of optical resonators such as whispering-gallery mode resonators [8,9] and photonic crystal cavities [10]. The nanotip may also be used as a scanning tip for weak-field sensing near surfaces. In magnetometry, for example, the field sensitivity will be determined by the atomic spin coherence time T_2. Coherence times of $T_2 \sim 1$ s yield ultimate magnetic field sensitivities of $\sim 20\ \text{pT}/\sqrt{\text{Hz}}$, which compare favorably with spins localized in solid state [26]. Furthermore, the tight trapping can yield novel atomic interactions. If two atoms are trapped simultaneously, the ground-state uncertainties can be made comparable to the typical range of their van der Waals interaction [27]. In this regime, optical forces could directly alter the molecular properties and dynamics. Arrays of nanotips could form optical lattices with very small lattice constants, enabling the exploration of novel many-body physics [28]. Finally, these ideas could be extended to other systems, such as polar molecules [2] or ions [23].

This work was supported by the NSF, Harvard-MIT CUA, DARPA, Packard Foundation, and the Gordon and Betty Moore Foundation through Caltech's Center for the Physics of Information, the Austrian Science Fund, and EU Projects.

[1] C. Monroe and M. D. Lukin, Phys. World **21**, 32 (2008).
[2] A. André, D. Demille, J. M. Doyle, M. D. Lukin, S. E. Maxwell, P. Rabl, R. J. Schoelkopf, and P. Zoller, Nature Phys. **2**, 636 (2006).
[3] R. Folman, P. Kruger, J. Schmiedmayer, J. Denschlag, and C. Henkel, Adv. At. Mol. Opt. Phys. **48**, 263 (2002).
[4] P. Treutlein, T. Steinmetz, Y. Colombe, B. Lev, P. Hommelhoff, J. Reichel, M. Greiner, O. Mandel, A. Widera, and T. Rom *et al.*, Fortschr. Phys. **54**, 702 (2006).
[5] D. E. Chang, A. S. Sørensen, P. R. Hemmer, and M. D. Lukin, Phys. Rev. B **76**, 035420 (2007).
[6] D. E. Chang, A. S. Sørensen, E. A. Demler, and M. D. Lukin, Nature Phys. **3**, 807 (2007).
[7] A. V. Akimov, A. Mukherjee, C. L. Yu, D. E. Chang, A. S. Zibrov, P. R. Hemmer, H. Park, and M. D. Lukin, Nature (London) **450**, 402 (2007).
[8] K. J. Vahala, Nature (London) **424**, 839 (2003).
[9] T. Aoki, B. Dayan, E. Wilcut, W. P. Bowen, A. S. Parkins, T. J. Kippenberg, K. J. Vahala, and H. J. Kimble, Nature (London) **443**, 671 (2006).
[10] J. Vučković and Y. Yamamoto, Appl. Phys. Lett. **82**, 2374 (2003).
[11] P. Treutlein, D. Hunger, S. Camerer, T. W. Hänsch, and J. Reichel, Phys. Rev. Lett. **99**, 140403 (2007).
[12] M. Righini, A. S. Zelenina, C. Girard, and R. Quidant, Nature Phys. **3**, 477 (2007).
[13] B. Murphy and L. V. Hau, Phys. Rev. Lett. **102**, 033003 (2009).
[14] R. Maiwald, D. Leibfried, J. Britton, J. C. Bergquist, G. Leuchs, and D. J. Wineland, arXiv:0810.2647.
[15] J. D. Jackson, *Classical Electrodynamics* (John Wiley & Sons, New York, 1999), 3rd ed.
[16] P. B. Johnson and R. W. Christy, Phys. Rev. B **6**, 4370 (1972).
[17] D. E. Chang, A. S. Sørensen, P. R. Hemmer, and M. D. Lukin, Phys. Rev. Lett. **97**, 053002 (2006).
[18] R. R. Chance, A. Prock, and R. Silbey, Phys. Rev. A **12**, 1448 (1975).
[19] J. M. McGuirk, D. M. Harber, J. M. Obrecht, and E. A. Cornell, Phys. Rev. A **69**, 062905 (2004).
[20] S. Groth, P. Krüger, S. Wildermuth, R. Folman, T. Fernholz, J. Schmiedmayer, D. Mahalu, and I. Bar-Joseph, Appl. Phys. Lett. **85**, 2980 (2004).
[21] This is consistent with preliminary experiments, where green laser light with intensities exceeding 10 $\text{mW}/\mu\text{m}^2$ has been found to not melt silver nanowires.
[22] C. Henkel, S. Pötting, and M. Wilkens, Appl. Phys. B **69**, 379 (1999).
[23] D. Leibfried, R. Blatt, C. Monroe, and D. Wineland, Rev. Mod. Phys. **75**, 281 (2003).
[24] D. J. Wineland and W. M. Itano, Phys. Rev. A **20**, 1521 (1979).
[25] R. A. Cline, J. D. Miller, M. R. Matthews, and D. J. Heinzen, Opt. Lett. **19**, 207 (1994).
[26] J. M. Taylor, P. Cappellaro, L. Childress, L. Jiang, D. Budker, P. R. Hemmer, A. Yacoby, R. Walsworth, and M. D. Lukin, Nature Phys. **4**, 810 (2008).
[27] E. L. Bolda, E. Tiesinga, and P. S. Julienne, Phys. Rev. A **66**, 013403 (2002).
[28] I. Bloch, J. Dalibard, and W. Zwerger, Rev. Mod. Phys. **80**, 885 (2008).